

- VAN DE HULST, H. C. 1957. Light scattering by small particles. Dover.
- VOLD, R. D., AND M. J. VOLD. 1966. Colloid chemistry, p. 263–265. *In* Encyclopedia of Chemistry. Reinhold.
- WAHLUND, K. G., AND A. LITZÉN. 1989. Application of an asymmetrical flow field-flow fractionation channel to the separation and characterization of proteins, plasmids, plasmid fragments, polysaccharides and unicellular algae. *J. Chromatogr.* **461**: 73–87.
- WELLS, M. L., AND E. D. GOLDBERG. 1991. Occurrence of small colloids in sea water. *Nature* **353**: 342–344.
- , AND ———. 1994. The distribution of colloids in the North Atlantic and Southern Oceans. *Limnol. Oceanogr.* **39**: 286–302.
- WILLIAMS, P. S., AND J. C. GIDDINGS. 1987. Power programmed field-flow fractionation: A new program form for improved uniformity of fractionating power. *Anal. Chem.* **59**: 2038–2044.
- ZSOLNAY, A. 1979. Coastal colloidal carbon: A study of its seasonal variation and the possibility of river input. *Estuar. Coast. Mar. Sci.* **9**: 559–567.

Received: 10 February 1999  
Accepted: 13 October 1999  
Amended: 31 October 1999

*Limnol. Oceanogr.*, 45(2), 2000, 492–498  
© 2000, by the American Society of Limnology and Oceanography, Inc.

## Light scattering by viral suspensions

*Abstract*—Viruses represent one of the most abundant, ocean-borne particle types and have significant potential for affecting optical backscattering. Experiments addressing the light-scattering properties of viruses have heretofore not been conducted. Here we report the results of laboratory experiments in which the volume-scattering functions of several bacterial viruses (bacteriophages) were measured at varying concentrations with a laser light-scattering photometer using a He-Ne and/or Argon ion laser (632.8 and 514.0 nm, respectively). Four bacterial viruses of varying size were examined, including the coliphages MS-2 (capsid size 25–30 nm) and T-4 (capsid size ~100 nm), and marine phages isolated from Saco Bay, Maine (designation Y-1, capsid size 50–80 nm) and Boothbay Harbor, Maine (designation C-2, capsid size ~110 nm). Volume-scattering functions (VSFs) were fitted with the Beardsley-Zaneveld function and then integrated in the backward direction to calculate backscattering cross section. This was compared to the virus geometric cross section as determined by transmission electron microscopy and flow-field fractionation. Typical backscattering efficiencies varied from  $20 \times 10^{-6}$  to  $1,000 \times 10^{-6}$ . Data on particle size and backscattering efficiencies were incorporated into Mie scattering calculations to estimate refractive index of viruses. The median relative refractive index of the four viruses was ~1.06. Results presented here suggest that viruses, while highly abundant in the sea, are not a major source of backscattering.

Radiative transfer in the ocean is driven by the optical properties of seawater, its suspended particles, and dissolved compounds. While the optical properties of pure sea water and particles  $>1 \mu\text{m}$  are reasonably well understood (Morel and Ahn 1991; Mobley 1994), the inherent optical properties (absorption and scattering) of submicron particles and dissolved matter are less well known, particularly in the micrometer to nanometer range. This size range includes the smallest algae, most bacteria, viruses, and colloids. In ocean optics, researchers have used a reductionistic approach to describe the inherent optical properties of the individual components. For example, phytoplankton are given one set

of specific absorption and scattering coefficients, while bacteria, which scatter more than they absorb, are given a different set of coefficients. This reductionistic approach to closure has revealed a large discrepancy between observed and predicted inherent optical properties, namely, when the optically scattering fractions are summed and compared to measured light scattering, only 50–75% of the total scattering can be accounted for by particles  $>0.5 \mu\text{m}$  (i.e., closure is not attained).

Experimental closure becomes even less attainable when one considers backscattered light, that is, the volume scattering integrated over all backward directions. Backscattering and absorption are important because they are used for predicting remote-sensing reflectance. Previous studies have shown that optical backscattering ( $b_b$ ) by the various particle types described above (all  $>0.5 \mu\text{m}$ ) represents an insignificant fraction of the total backscattering coefficient, accounting for ~10% of the total  $b_b$  (Morel and Ahn 1991; Stramski and Kiefer 1991). Models have suggested that 3- $\mu\text{m}$  particles are responsible for most of the total light scattering in the ocean, with particles  $\leq 0.1 \mu\text{m}$  responsible for the bulk of the backscattering coefficient (Morel and Ahn 1991; but note that Stramski and Kiefer [1991] were less restrictive and suggested that most backscattering came from particles  $<1 \mu\text{m}$ ). Particles smaller than  $0.1 \mu\text{m}$  would be considered dissolved given the operational definition of dissolved organic matter (i.e., anything passing through a 0.2- $\mu\text{m}$  filter). The composition of these particles is unknown, but may include colloidal particles smaller than  $0.6 \mu\text{m}$ , such as Koike particles (Koike et al. 1990), microgels (Chin et al. 1998), or viruses.

Viruses represent an abundant, diverse, and important component of the suspended matter in the world ocean (Boersheim et al. 1990; Hara et al. 1991), with concentrations ranging from  $10^6$  to as high as  $10^{14} \text{ m}^{-3}$  in eutrophic regions (Bergh et al. 1989; Kepner et al. 1998). Viruses infect all members of the marine plankton and are thought to play an important role in the ecological control of planktonic microorganisms (Proctor and Fuhrman 1990;

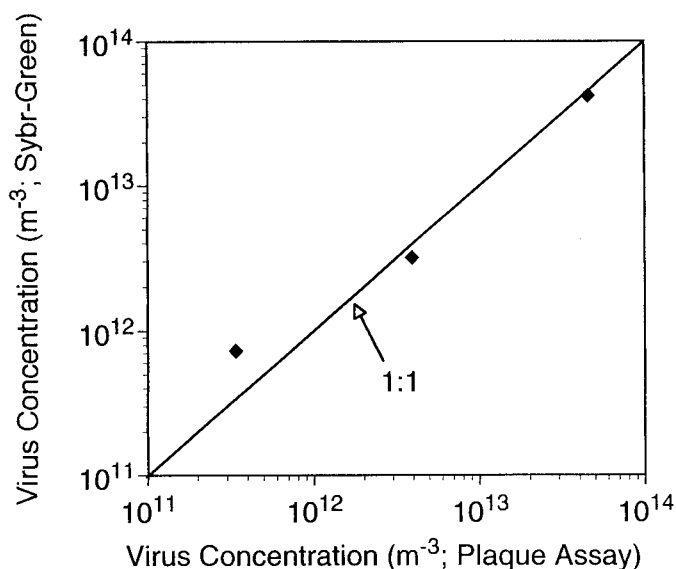


Fig. 1 C2 virus concentration estimated with two techniques, Sybr-green (Noble and Fuhrman 1998) and plaque assay (Adams 1959). Best fit equation to the data was  $Y = a(X^{0.85})$  where  $a = \exp(2.45)$ ;  $r^2 = 0.968$ .

Suttle and Chan 1993). Although bacterioplankton and phytoplankton represent the most ubiquitous and abundant hosts for viral infection in sea water, it has been suggested that nearly all oceanic life forms harbor viral pathogens.

As a group, viruses present several morphological types: (1) icosohedral—resembling crystals; (2) helical—the nucleic acid is surrounded by a cylindrical capsid; (3) enveloped—the nucleocapsid is surrounded by lipid (usually host derived); and (4) complex—including those without an identifiable capsid, but containing several protein coats, and certain bacterial viruses that possess additional structures such as a tail. Most of the viruses from marine waters have been shown to possess either helical or icosohedral symmetry, with about 50% of the latter containing short or long tails, or other appendages. Marine virus particles range in size from <30 nm (capsid size) to 750 nm (Bratbak et al. 1992). The most ubiquitous groups in the euphotic and aphotic zones of the open ocean appear to be made up of particles having a capsid size of 30 to 85 nm (Cochlan et al. 1993).

In the present study, we investigated the role of viruses in accounting for the missing backscattering by serially diluting purified virus particles and measuring their volume-scattering properties. The objectives of this study were to understand the optical properties of (1) two common enteric viruses, and (2) two marine bacteriophages. The results are directly applicable to bio-optical models.

**Materials and methods**—Propagation, purification, and enumeration of viruses: Viruses were propagated on bacterial host cultures. Experiments were performed in which four types of phage were propagated to concentrations of  $10^8$  to  $10^{10}$  viruses  $\text{ml}^{-1}$ . These phages were dramatically different in size and morphology. Coliphages and their appropriate

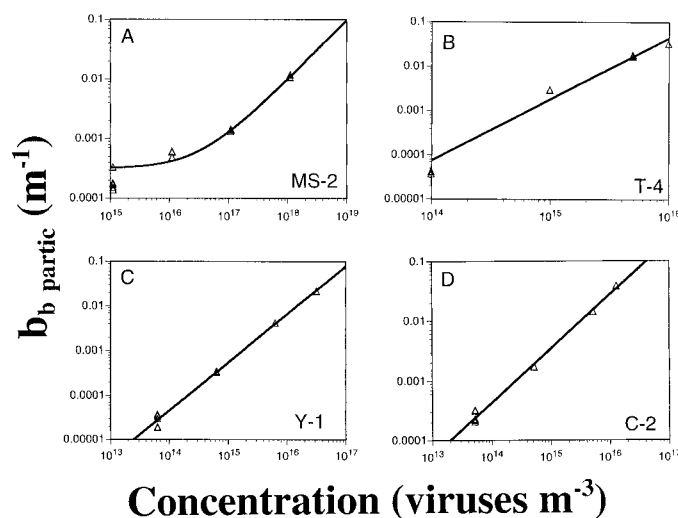


Fig. 2 Results of dilution experiment with four marine viruses: (A) MS2 dilution in filtered sea water, best fit  $Y = 0.965 \times 10^{-21} X + 0.313 \times 10^{-4}$ ,  $r^2 = 0.997$ ; (B) T4 dilution in PBS buffer, best fit  $Y = 3.342 \times 10^{-12} X - 9.322 \times 10^{-5}$ ,  $r^2 = 0.998$ ; (C) Y-1 dilution in filtered seawater, best fit  $Y = 6.821 \times 10^{-19} X - 8.027 \times 10^{-5}$ ,  $r^2 = 0.9999$ ; (D) C2 dilution in PBS, best fit  $Y = 9.899 \times 10^{-17} X^{0.9025}$ ;  $r^2 = 0.9956$ . In all experiments, purified virus was diluted serially and the backscattering from the blanks have been subtracted so that the ordinate provides particulate backscattering ( $b_{b \text{ partic}}$ ).

host cells were obtained from the American Type Culture Collection (ATCC). The first viral strain tested was MS2 (ATCC 15597 B-1, host cell, *Escherichia coli* ATCC 15597), a small, icosohedral virus (25–30 nm) containing single-stranded RNA. The second phage studied was T4 (ATCC 11303 B-1, host cell, *E. coli* ATCC 11303), a 100-nm double-stranded DNA phage (including an elongated capsid and tail structure). We also isolated two strains of marine virus, one from waters off of Saco Bay, Maine, designated Y1 (capsid 50–80 nm), and another from waters off the Bigelow Laboratory dock, designated C2 (capsid 110 nm).

*E. coli* host stocks were propagated in tryptone yeast extract broth (TYEB composition: tryptone 10 g  $\text{L}^{-1}$ , yeast extract 1.0 g  $\text{L}^{-1}$ , glucose 1.0 g  $\text{L}^{-1}$ , NaCl 9.0 g  $\text{L}^{-1}$ , CaCl 0.22 g  $\text{L}^{-1}$ ). Short-term storage of host cultures involved the preparation of cultures on tryptone agar slants. For long-term storage, 18 h host cultures propagated in TYEB were supplemented with 10% sterile glycerol, dispensed as 1-ml aliquots in cryovials, and stored at  $-74^\circ\text{C}$ . MS2 and T4 stocks were prepared in a similar manner. Overnight cultures of respective host cells were inoculated into TYEB and incubated with shaking for 2 h. One-milliliter aliquots of appropriate phage stock ( $10^9$ – $10^{10}$  plaque-forming units [pfu]  $\text{ml}^{-1}$ ) were then added, and incubation continued for an additional 4 h. Cultures were then centrifuged (5,000 g/15 min) to remove debris, and further clarified via filtration (0.22  $\mu\text{m}$ ). Resulting bacteriophage titers, enumerated by plaque assay (Adams 1959), averaged  $10^{11}$  pfu  $\text{ml}^{-1}$  for MS2 and  $10^{10}$  pfu  $\text{ml}^{-1}$  for T4. Phage stocks were stored in 1-ml aliquots at  $-74^\circ\text{C}$ .

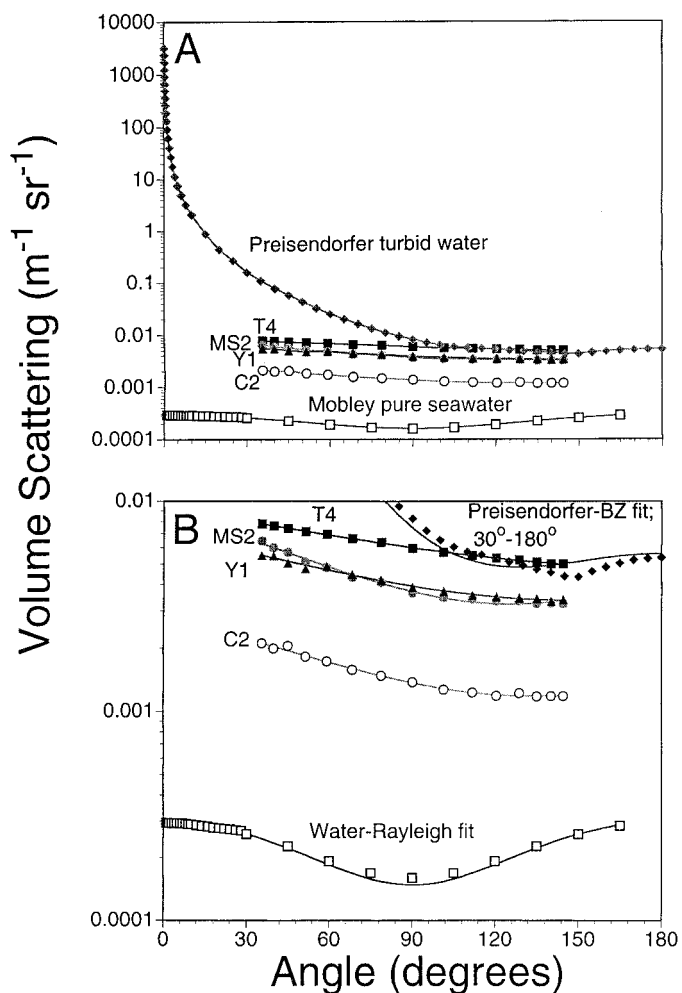


Fig. 3 (A) Shapes of volume-scattering functions for four different viruses, MS2 (*E. coli* virus; solid circles), T4 (*E. coli* virus; triangles), Y1 (marine bacteriophage; squares), and C2 (marine bacteriophage; open circles). The sizes of these different viruses are 25–30 nm, 100 nm, 50–80 nm, and 110 nm respectively. Note, volume scattering ( $Y$  axis) is a log scale, and the VSFs are relatively flat compared to typical VSFs found for larger marine particulate matter (Mobley 1994). (B) Same results as (A), but with expanded ordinate scale to show lack of symmetry for VSFs. Lines represent least-square fits to the data using the following equations: Preisendorfer Turbid water data fitted with Beardsley-Zaneveld equation:  $Y = 7.45 \times 10^{-3} \{1 / [1 - (7.521 \times 10^{-1} [\cos X])^4] \times [1 + (0.388 [\cos X])^4]\}$ ;  $r^2 = 0.999$ . MS2 fitted to polynomial:  $Y = 3.618 \times 10^5 ([1.045 \times 10^2 \times X^2] + [2.616X] + 2.5307 \times 10^2)$ ;  $r^2 = 0.992$ . T4 fitted to polynomial:  $Y = 4.137 \times 10^5 ([3.332 \times 10^3 \times X^2] + [1.220X] + 2.273 \times 10^2)$ ;  $r^2 = 0.999$ . Y1 fitted to polynomial:  $Y = 2.988 \times 10^5 ([5.805 \times 10^3 \times X^2] + [1.698X] + 2.372 \times 10^2)$ ;  $r^2 = 0.988$ . C2 fitted to polynomial:  $Y = 1.254 \times 10^5 ([7.723 \times 10^3 \times X^2] + [2.064X] + 2.321 \times 10^2)$ ;  $r^2 = 0.991$ . Pure water using Rayleigh fit:  $Y = 1.483 \times 10^4 \{1 + [(\cos X)^2]\}$ ;  $r^2 = 0.998$ .

Marine bacteriophage and host cells were isolated from 2–3-liter water samples collected from Saco Bay or West Boothbay Harbor, Maine. Briefly, candidate host bacteria were isolated using a membrane filtration method. Mem-

branes were placed on pads containing 2216 Marine Broth (Difco) and incubated overnight at 25°C. Resulting colonies were picked and grown overnight as pure cultures in 2216 broth. Phage isolation involved an enrichment technique. Overnight cultures (100 ml) of candidate host cultures were concentrated by centrifugation ( $5,000 \times g$  for 15 min), re-suspended in 5-ml 2216 broth, and inoculated into 500-ml flasks containing triple strength 2216 broth (100 ml) and 300 ml of the original water sample from which the candidate host had been isolated. Enrichment flasks were incubated (25°C) with shaking for 1–3 d. Following this, 5-ml aliquots from each enrichment were filtered ( $0.22 \mu\text{m}$ ), spot tested on lawns of original host cell, and observed for the development of typical virus plaques over a 24–48 h period. Of the several phage types isolated, a subset was selected for further study by virtue of their rapid lysis (6–12 h) of host cell. Selected phage lysates were stored frozen as described above. Average lysate phage titers were  $10^9$  pfu  $\text{ml}^{-1}$ .

Purified, high titer, phage stocks used in optical experiments were prepared in the following manner. Overnight host cell cultures were inoculated into 1-liter volumes of TYEB and incubated with shaking for 2–3 h. Cultures were then inoculated with  $10^9$  to  $10^{10}$  pfu of appropriate bacteriophage and incubation continued for 4–12 h. Lysates were centrifuged and clarified as previously described, and the virus concentrated by ultracentrifugation ( $230,000 \times g$  for 2 h). Resulting pellets were resuspended in 4 ml of phosphate buffered saline (PBS composition:  $\text{KH}_2\text{PO}_4$  0.144 g  $\text{L}^{-1}$ ,  $\text{NaCl}$  9.0 g  $\text{L}^{-1}$ ,  $\text{Na}_2\text{HPO}_4$  0.795 g  $\text{L}^{-1}$ ), layered onto cesium chloride gradients (1.3–1.7 g  $\text{ml}^{-1}$ ), and centrifuged ( $100,000 \times g$  for 60 min at 10°C; Bachrach and Freidman 1971). Resulting virus bands were collected and dialyzed overnight (4°C) against half-strength PBS. Purified, concentrated virus stocks were assayed and stored at 4°C until used. Phage concentrations in purified stocks averaged  $\sim 10^{12}$  pfu  $\text{ml}^{-1}$  for MS2,  $10^{10}$  pfu  $\text{ml}^{-1}$  for T4,  $10^{11}$  pfu  $\text{ml}^{-1}$  for Y1 phage, and  $10^{12}$  pfu  $\text{ml}^{-1}$  for C2 phage.

Size distribution measurements: For calculation of absorption, scattering, and backscattering efficiencies, one needs to know the optical, as well as physical cross sections of the particles. Owing to the small size of virus particles, Coulter counting cannot be effectively used to estimate the size spectrum of a virus suspension. The most effective means to acquire such a size spectrum is with transmission electron microscopy and/or field-flow fractionation (FFF); examples of this technique applied to aqueous particle suspensions can be found elsewhere (Beckett and Hart 1993; Vaillancourt and Balch 2000). This is a chromatographic-like separation that occurs in a thin ribbon-shaped channel as an external field and/or pressure gradient is applied perpendicularly to the flow channel. Typically used gradients for fractionation are sedimentation, thermal, or cross flow. FFF allows fractionation of materials from a few thousand molecular weight to 100- $\mu\text{m}$  particle diameters, but our experience has shown that submicron particles are sorted the best. FFF has been used previously to size fractionate viruses (Giddings et al. 1980). In the context of these experiments, FFF allows separation of viral aggregates and membrane

Table 1. Mean backscattering cross-sections for four virus types, calculated from individual values of  $b_b$  ( $\text{m}^{-1}$ ) per unit concentration (viruses  $\text{m}^{-3}$ ). Each experiment typically had at least four concentrations examined. Average backscattering efficiencies also calculated as the backscattering cross-section normalized to the physical cross-section. Mie calculations were made according to Bohren and Huffman (1983). When a range of virus sizes was observed (e.g., MS2 and Y1) then a minimum and maximum expected refractive index was calculated; otherwise, only one refractive index was estimated. Abbreviations used for the Mie scattering calculations:  $n(\text{rel})$  = real refractive index relative to the medium (PBS or FSW), subscript "min" indicates the minimum  $n$  value corresponding to maximum virus diameter, and subscript "max" indicates the maximum  $n$  value corresponding to minimum virus diameter. Results from the first MS2 experiment in PBS (marked with an asterisk) should be interpreted cautiously due to the high refractive index derived from Mie calculations (considerably higher than expected for organic particles).

Virus	Diameter capsid (nm)	Diluant	$\lambda$ (nm)	Mean $b_b^*$ ( $\times 10^{-20} \text{ m}^2 \text{ virus}^{-1}$ )		SD ( $\times 10^{-20} \text{ m}^2 \text{ virus}^{-1}$ )		Min ( $\times 10^{-20} \text{ m}^2 \text{ virus}^{-1}$ )		Max ( $\times 10^{-20} \text{ m}^2 \text{ virus}^{-1}$ )		Physical cross section ( $\times 10^{-20} \text{ m}^2 \text{ virus}^{-1}$ )	$Q_{\text{backsc}} (\times 10^{-6})$	SD ( $\times 10^{-6}$ )	$n(\text{rel})_{\text{min}}$	$n(\text{rel})_{\text{max}}$
				SD	Min	Max	SD	SD								
MS2	25–30	PBS*	633	4.62	1.25	1.25	2.19	6.57	59400	77.8	21.0	1.177	1.257			
		FSW	514	1.13	0.15	0.97	1.31	2.58	1.165							
T4	100	PBS	633	241	150	nd	366	$1.54 \times 10^6$	157	97.4	1.026					
		FSW	514	586	3.22	581	590	2.09	381	2.09	1.029					
Y1	50–80	PBS	514	329	26.8	294	365	$3.32 \times 10^5$	991	80.8	1.067	1.156				
		FSW	514	285	32.2	252	327	859	97	1.061	1.143					
C2	110	PBS	514	337	156	nd	495	$9.50 \times 10^5$	355	164	1.025					
		FSW	514	583	322	368	1,290	614	339	1.032						

fragments from solitary viruses for subsequent optical measurements.

Optical measurements: A Dawn laser light-scattering photometer (Wyatt Technologies) was used for measuring the volume-scattering function and the calculation of the backscattering coefficient ( $b_b$ ). This instrument measures the volume-scattering function at a rate of 400 Hz and averages the data over any preset time period. The light-scattering photometer initially was equipped with a helium neon laser (632.8 nm), then upgraded to an argon ion laser light source (514.0 nm). Discrete samples were placed in a cylindrical 2.7 cm diameter glass cuvette. This instrument measured the volume-scattering function at 15 angles between 35.5 and 144.5°, plus at 0° with a precuvette and postcuvette laser monitor. Volume-scattering data were fit to the Beardsley-Zaneveld function, which was then integrated in the backward direction in order to calculate total backscattering. Detector calibration was performed with a factory-supplied standard (a polished solid glass cylinder with beads suspended within), which scatters ~6 times more than toluene. The 90° detector is first calibrated, then the other detectors are intercalibrated (or normalized) by virtue of the isotropic scattering from the standard. More details of the Wyatt Dawn light-scattering photometer can be found in Balch et al. (1999; see the legend to their table 2).

Purified virus stocks were serially diluted and assayed to verify the concentration dependence of viruses on their volume-scattering properties. The Sybr-green technique (Noble and Fuhrman 1998) was used on several occasions to cross check virus and bacterial concentrations, estimated by standard plaque assays and plate counts, respectively. Initial experiments with MS2 and T4 were conducted in phosphate buffered saline (pH 7.2). Once absorption and scattering characteristics were established, serial dilution experiments were repeated in ultrafiltered sea water from the Gulf of Maine into which known titers of the above viruses were inoculated.

*Results and discussion*—The backscattering cross section for the four viruses of varying morphology was quantified in these experiments. Parallel estimates of virus concentration using plaque assays and the Sybr-green techniques showed similar good agreement (Fig. 1), which suggests that most of the viruses stained by Sybr-green were infectious. Serial dilution experiments demonstrated viral impact on backscattering at the upper end of the concentration range reported for seawater. In addition, the linearity of backscattering versus dilution plots was strong (Fig. 2; note that the line in Fig. 2A is curved due to plotting on log-log axes, with nonzero  $Y$  intercept). All VSFs were distinctly flatter than typical VSFs for suspensions of particles  $>1 \mu\text{m}$ . However, the shapes of the VSFs were not symmetrical for the four viral types, lacking a minimum at 90°, as predicted by the equation for volume scattering by Rayleigh particles ( $\beta_{\text{Ray}}$ ; Mobley 1994; Fig. 3).

$$\beta_{\text{Ray}}(\theta; \lambda) = \beta_{\text{Ray}}(90^\circ; \lambda_o)(\lambda_o/\lambda)^4 (1 + \cos 2\theta) \quad (1)$$

In the above equation,  $\lambda_o$  represents a reference wavelength,  $\lambda$  represents the wavelength of interest, and  $\theta$  rep-

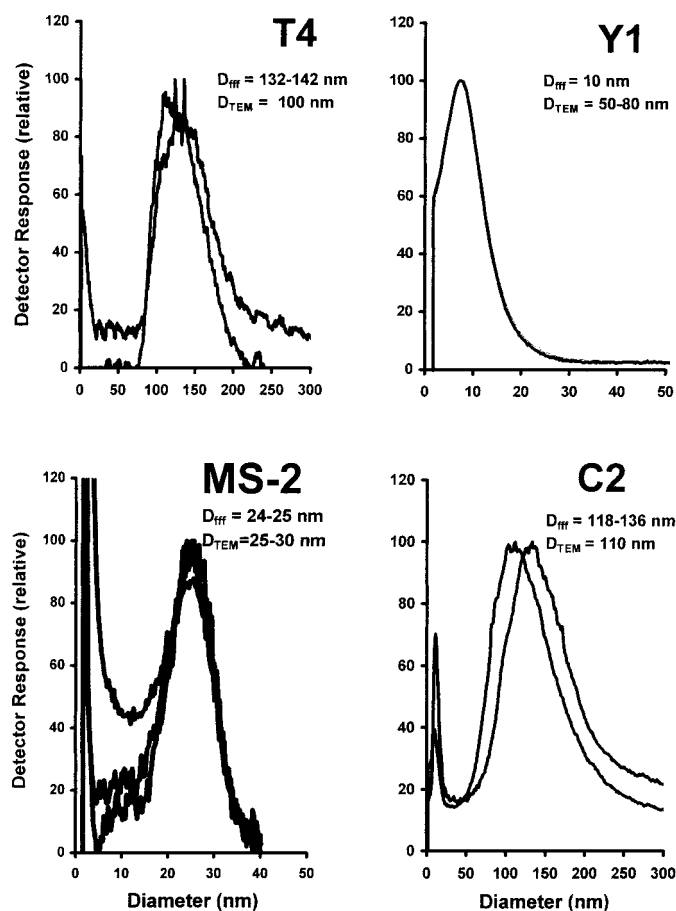


Fig. 4 Flow-field fractionation plots of four virus strains. Peaks at sizes  $<5$  nm are likely artifactual from initial void peak. The virus separation involved an injection of  $20 \mu\text{l}$  of virus concentrate and the carrier solution was PBS (pH 7.2) except for C2 virus injection, which used boric acid-buffered saline (pH 9.5) as carrier. The surfactant Pluronic F68 (BASF) was added to all carrier solutions to a final concentration of 0.1%. All fractionations were done with a regenerated cellulose membrane with Channel flow =  $1.9 \text{ ml min}^{-1}$ , and constant cross flow =  $0.92 \text{ ml min}^{-1}$ . The determination of absolute size was based on calibration beads, blank baselines, and eqs. 1–3 in Vaillancourt and Balch (1999). The peak diameter based on flow-field fractionation ( $D_{ff}$ ) is shown along with the diameter based on transmission electron microscopy ( $D_{TEM}$ ). With Y-1, the triplicate runs lay exactly over one another, but the difference between  $D_{TEM}$  and  $D_{ff}$  is significant, suggesting that there may have been nonideal particle interaction with the cellulose membrane during the flow-field fractionation (see Vaillancourt and Balch 1999). Owing to this observation, the FFF data for Y-1 should be used with caution.  $D_{TEM}$  was used in all subsequent Mie calculations.

resents the scattering angle. The viral VSFs were best fit by second-order polynomials, although we cannot ascribe any physico-optical interpretation to these curves. Caution should be used when extrapolating volume scattering with these polynomials outside of the angles measured in this study.

It should be noted that the backscattering cross sections (Table 1) were consistent with published values based on

Mie scattering model calculations (Stramski and Mobley 1997). The relative refractive indices for the eight viral suspensions also were determined by iterative Mie scattering calculations of backscattering efficiency for homogeneous spheres (Bohren and Huffman 1983). Known values of viral capsid radius, medium refractive index and wavelength, plus a range of plausible viral refractive indices, were used as input to the model. The viral refractive index reported here was that which returned values of  $Q_{bb}$  equivalent to the experimentally determined value. Assumptions inherent in this determination were homogenous particle composition and sphericity. The Mie-calculated refractive indices for these particles were largest for the smallest viruses. Relative refractive index values for T4, C2, and Y1 (1.02–1.07) were typical of living organic matter (1.01–1.09), while MS2 in PBS had relative refractive index values more similar to detrital and inorganic particles (1.15–1.2; Jerlov 1976; Mobley 1994). We know of no biochemical difference that would give MS2 in PBS the greater relative refractive index, and can only attribute differences between observations and Mie-scattering modeling to (1) possible experimental error in any of the three measurements (volume scattering, viral abundance, or viral size) or (2) the Mie scattering model for homogeneous spheres may not have adequately represented the structure of the MS2 virus. Nevertheless, for the other virus strains, the range of relative refractive index values calculated from our empirical measurements, combined with Mie scattering calculations, was reasonably close to the value assumed by Stramski and Kiefer (1991) of 1.05.

Wavelength dependence of backscattering only can be confidently deduced from one of the virus strains used in our experiments (T4), and unfortunately the measurements at different wavelengths also were in two different media (PBS or filtered seawater), so the wavelength differences shown in Table 1 should be interpreted cautiously. Based on Mie scattering calculations, the wavelength dependence of backscattering by homogeneous spheres of 50-nm radius (equivalent spherical radius of T4 viruses) should be  $\sim\lambda^{-3.1}$ . This was lower spectral dependence than we observed in experiments ( $\lambda^{-4.27}$ ; Table 1). As with the above, any differences between Mie predictions and real measurements can be attributed to experimental error, particle shape, or composition. Mie-predicted wavelength dependence for MS2, Y1, and C2 was  $\sim\lambda^{-3.9}$ ,  $\sim\lambda^{-3.5}$ , and  $\sim\lambda^{-2.9}$ , respectively.

Viral aggregates probably were not an issue in the interpretation of these results since flow-field fractionation demonstrated viral particles were mostly solitary (i.e., the particle spectrum for our virus suspensions generally showed the major mode at the same size as the viruses observed with transmission electron microscopy; Figs. 4, 5). Thus, contamination by other colloids was probably not a problem unless the colloids were the same size as the viruses, such that they always overlapped in the fractograms (which would have been unlikely).

These results are of use in understanding the overall role of viruses in the sea and in addressing the hypothesis of Morel and Ahn (1991), which suggested that viruses might represent a significant fraction of the missing backscattering in the sea. At present, we would concur with the modeling results of Stramski and Kiefer (1991) that viruses, while a significant source of backscattering, are not responsible for

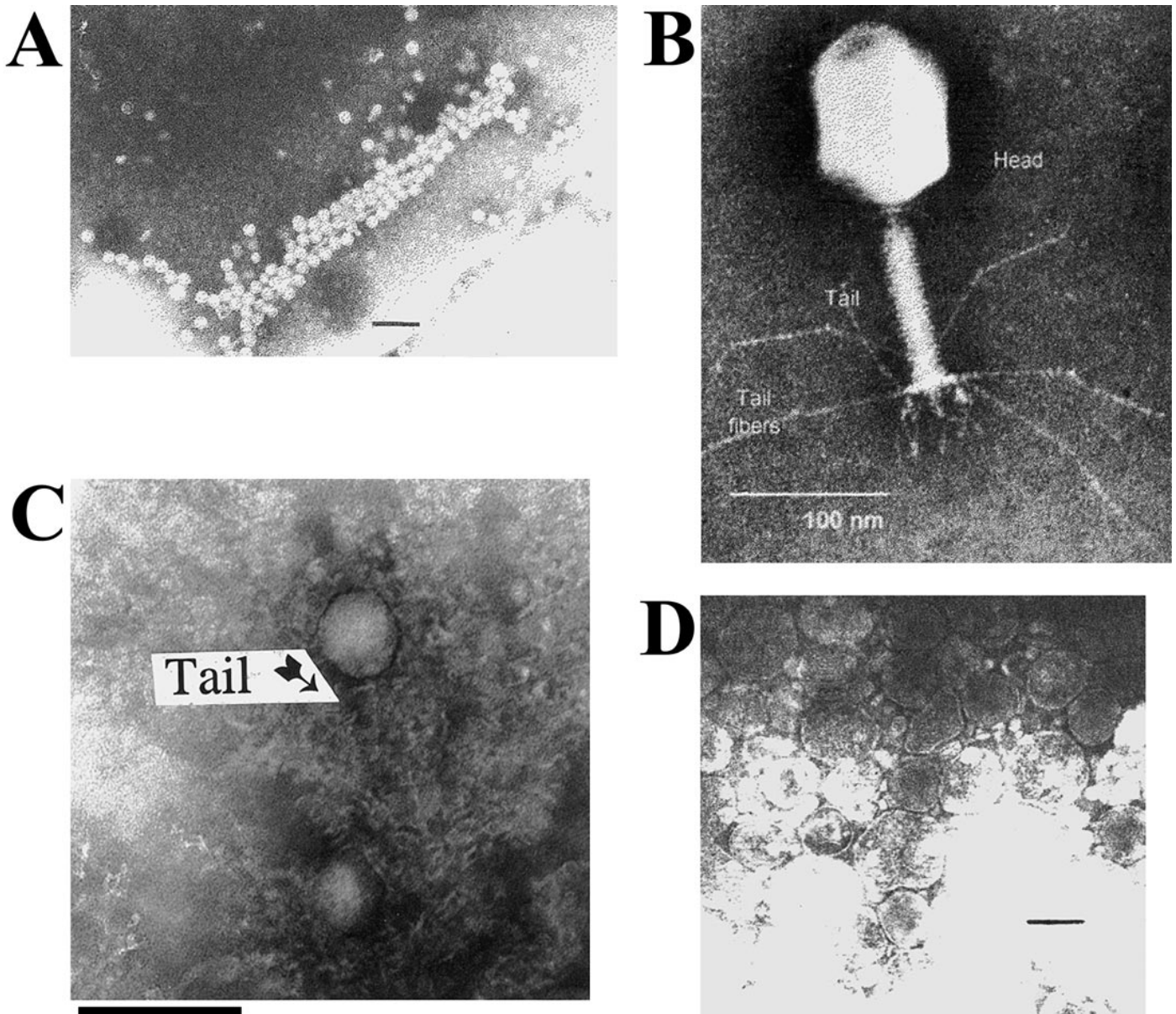


Fig. 5 Transmission electron micrographs of (A) MS2 levivirus (source: <http://life.anu.edu.au/viruses/WIntkey/Images/089-30.jpg>); (B) T4 virus (source: <http://life.anu.edu.au/viruses/WIntkey/Images/em.t4.gif>); (C) Y1 bacteriophage (D) C2 bacteriophage (Scale bars = 100 nm).

the bulk of the missing backscattered light. Measured backscattering cross sections for T4 phage, a 100-nm virus (Figs. 4, 5), were about  $2\text{--}5 \times 10^{-18} \text{ m}^2 \text{ virus}^{-1}$  (Table 1). Thus, at typical virus seawater concentrations of  $1 \times 10^{13} \text{ m}^{-3}$  (Bratbak et al. 1995; Brussaard et al. 1996; Nobel and Fuhrman 1998), they would cause backscattering of  $2\text{--}5 \times 10^{-5} \text{ m}^{-1}$ , which represents 0.2 to 2% of the total backscattering observed in mesotrophic to eutrophic waters of the Gulf of Maine (Balch unpubl. data). This would be the same amount of scattering contributed by phytoplankton and heterotrophic bacteria in oligotrophic waters containing  $0.04 \text{ mg Chl } a \text{ m}^{-3}$ , but far from the  $0.4\text{--}2.0 \times 10^{-3} \text{ m}^{-1}$  backscattering required for optical closure in coastal waters (Morel and Ahn 1991).

The finding that viruses by themselves do not represent a major source of backscattered light does not mean that they can be dismissed as optically unimportant. Their principle optical impact may be related to their rapid infection and lysis of larger, optically active cells. Virus-induced particle degeneration into submicron Rayleigh scatterers may be a major source of the missing backscattering. It has become increasingly apparent that bloom dynamics can be strongly modulated by viruses. For example, in a North Sea *Emiliania huxleyi* bloom, up to 50% of the cells were infected by viruses at the end of the bloom (Bratbak et al. 1995). Moreover, virus-induced lysis of *E. huxleyi* cells resulted in the apparent release of large quantities of dissolved organic carbon in the bloom (Brussaard et al. 1996; see also Fuhrman

1992 for a general discussion of virally mediated release of dissolved organic matter). These observations agree with a model (Fuhrman and Suttle 1993) in which both bacteria and phytoplankton were infected by viruses, such that when 10% of the host phytoplankton were infected, their lysis, with subsequent release of dissolved organic carbon into the media, would increase bacterial production by one-third. Virus destruction of optically active hosts will likely release DOC and affect the optical properties of the suspension as the particle size distribution changes.

*William M. Balch*

Bigelow Laboratory for Ocean Sciences  
P.O. Box 475  
West Boothbay Harbor, Maine 04575

*James Vaughn  
James Novotny*

Department of Microbiology  
College of Osteopathic Medicine  
University of New England  
Biddeford, Maine 04005

*David T. Drapeau  
Robert Vaillancourt*

Bigelow Laboratory for Ocean Sciences  
P.O. Box 475  
West Boothbay Harbor, Maine 04575

*Janeen Lapierre*

Department of Microbiology  
College of Osteopathic Medicine  
University of New England  
Biddeford, Maine 04005

*Amanda Ashe*

Bigelow Laboratory for Ocean Sciences  
P.O. Box 475  
West Boothbay Harbor, Maine 04575

## References

- ADAMS, M. H. 1959. Bacteriophages, Interscience.
- BACHRACH, U., AND A. FREIDMAN. 1971. Practical procedures for the purification of bacterial viruses. *Appl. Microbiol.* **22**: 706–715.
- BALCH, W. M., D. T. DRAPEAU, T. L. CUCCI, AND R. D. VAILLANCOURT, K. A. KILPATRICK, AND J. J. FRITZ. 1999. Optical backscattering by calcifying algae—separating the contribution by particulate inorganic and organic carbon fractions. *J. Geophys. Res.* **104**: 1541–1558.
- BECKETT, R., AND B. T. HART. 1993. Use of field-flow fractionation techniques with aquatic particles, colloids and macromolecules, vol. 2, p. 165–205. *In* J. Buffle and H. P. van Leeuwen [eds.], *Environmental particles*. CRC.
- BERGH, O., K. Y. BOERSHEIM, G. BRATBAK, AND M. HELDAL. 1989. High abundance of viruses found in aquatic environments. *Nature* **340**: 467–468.
- BOERSHEIM, K. Y., G. BRATBAK, AND M. HELDAL. 1990. Enumeration and biomass estimation of planktonic bacteria and viruses by transmission electron microscopy. *Appl. Environ. Microbiol.* **56**: 352–356.
- BOHREN, C. F., AND D. R. HUFFMAN. 1983. Absorption and scattering of light by small particles. Wiley.
- BRATBAK, G., O. H. HASLUND, M. HELDAL, A. NOESS, AND T. R. ROEGGEN. 1992. Giant marine viruses? *Mar. Ecol. Progr. Ser.* **85**: 201–202.
- , M. LEVASSEUR, S. MICHAUD, G. CANTIN, E. FERNANDEZ, B. HEIMDAL, AND M. HELDAL. 1995. Viral activity in relation to *Emiliania huxleyi* blooms: A mechanism of DMSP release? *Mar. Ecol. Progr. Ser.* **128**: 133–142.
- BRUSSAARD, C. P. D., R. S. KEMPERS, A. J. KOP, R. RIEGMEN, AND M. HELDAL. 1996. Virus-like particles in a summer bloom of *Emiliania huxleyi* in the North Sea. *Aquat. Microb. Ecol.* **10**: 105–113.
- CHIN, W. C., M. V. ORELLANA, AND P. VERDUGO. 1998. Spontaneous assembly of marine dissolved organic matter into polymer gels. *Nature* **391**: 568–572.
- COCHLAN, W. P., J. WIKNER, G. F. STEWARD, D. C. SMITH, AND F. AZAM. 1993. Spatial distribution of viruses, bacteria and chlorophyll *a* in neritic, oceanic and estuarine environments. *Mar. Ecol. Progr. Ser.* **92**: 77–87.
- FUHRMAN, J. 1992. Bacterioplankton roles in cycling of organic matter: The microbial food web, p. 361–383. *In* P. G. Falkowski and A. D. Woodhead [eds.], *Primary productivity and biogeochemical cycles in the sea*. Plenum.
- , AND C. A. SUTTLE. 1993. Viruses in marine planktonic systems. *Oceanography* **6**: 51–63.
- GIDDINGS, J. C., M. N. MYERS, K. D. CALDWELL, AND S. R. FISHER. 1980. Analysis of biological macromolecules and particles by field-flow fractionation, p. 79–136. *In* D. Glick [ed.], *Methods of biochemical analysis*, Vol. 26. Wiley.
- HARA, S., K. TERAUCHI, AND I. KOIKE. 1991. Abundance of viruses in marine waters: Assessment by epifluorescence and transmission electron microscopy. *Appl. Environ. Microbiol.* **56**: 352–356.
- JERLOV, N. G. 1976. *Marine optics*. Elsevier.
- KEPNER, R. L., R. A. WHARTON, JR., AND C. A. SUTTLE. 1998. Viruses in Antarctic lakes. *Limnol. Oceanogr.* **43**: 1754–1761.
- KOIKE, I., S. HARA, K. TERAUCHI, AND K. KOGURE. 1990. Role of sub-micrometer particles in the ocean. *Nature* **345**: 242–244.
- MOBLEY, C. D. 1994. Light and water—radiative transfer in natural waters. Academic.
- MOREL, A., AND Y. AHN. 1991. Optics of heterotrophic nanoflagellates and ciliates: A tentative assessment of their scattering role in oceanic waters compared to those of bacterial and algal cells. *J. Mar. Res.* **49**: 177–202.
- NOBLE, R. T., AND J. A. FUHRMAN. 1998. Use of SYBR Green I for rapid epifluorescence counts of marine viruses and bacteria. *Aquat. Microb. Ecol.* **14**: 113–118.
- PROCTOR, L. M., AND J. A. FUHRMAN. 1990. Viral mortality of marine bacteria and cyanobacteria. *Nature* **343**: 60–62.
- STRAMSKI, D., AND D. A. KIEFER. 1991. Light scattering by microorganisms in the open ocean. *Prog. Oceanogr.* **28**: 343–383.
- , AND C. D. MOBLEY. 1997. Effects of microbial particles on oceanic optics: A database of single-particle optical properties. *Limnol. Oceanogr.* **42**: 538–549.
- SUTTLE, C. A., AND A. M. CHAN. 1993. Marine cyanophages infecting oceanic and coastal strains of *Synechococcus*: Abundance, morphology, cross-infectivity and growth characteristics. *Mar. Ecol. Progr. Ser.* **92**: 99–109.
- VAILLANCOURT, R. D., AND W. M. BALCH. 2000. Size distribution of coastal sub-micron particles determined by flow, field flow fractionation. *Limnol. Oceanogr.* **45**: 485–492.

## Acknowledgements

We wish to acknowledge Robert Andersen (Bigelow Laboratory for Ocean Sciences) for help with transmission electron microscopy. This work was funded by the Office of Naval Research (grant numbers N00014-96-1-0999 and N00014-99-1-0645 to J.M.V. and W.M.B.). This is contribution number 99007 of the Bigelow Laboratory for Ocean Sciences.

*Received: 22 March 1999  
Accepted: 9 November 1999  
Amended: 9 November 1999*